Electric Power Systems Research 211 (2022) 108234

Contents lists available at ScienceDirect

Electric Power Systems Research

journal homepage: www.elsevier.com/locate/epsr

Influence of the wind variability on the calculation of dynamic line rating

M.Á. González-Cagigal [a,*], J.A. Rosendo-Macías [a], A. Bachiller-Soler [a], D. Señas-Sanvicente [b]

[a] Department of Electrical Engineering, University of Seville, Seville, Spain
[b] Ingelectus S.L., Seville, Spain

ARTICLE INFO

Keywords:
Dynamic line rating
Electrical clearance
Monte Carlo
Overhead transmission lines

ABSTRACT

This paper presents a novel technique to calculate the ampacity of an overhead transmission line in real time, considering the dynamic evolution of the conductor temperature. In case this method cannot be applied due to lack of adequate information, a correction is proposed for the maximum current, based on Monte Carlo simulations assuming unfavorable external conditions, and validated with real data from a weather station. This technique might be used to avoid the temporary violation of the minimum electrical clearance in transmission lines.

1. Introduction

The optimization of the transmission utilities is a prevailing challenge in the operation and control of electric power systems. In the particular case of overhead transmission lines (OHTLs), and due to the increasing electricity demand and the arising of new generation plants, it is important to accurately establish the capacity of the conductor in order to reduce infrastructure expansion and the corresponding economic outlay.

The ampacity (or rating) of OHTLs is defined as the maximum current that can circulate through the conductor without causing overheating and its derived problems, like an excessive sag, [1], or conductor damage, [2].

A traditional approach is the so-called static line rating (SLR), where an ampacity is calculated for long periods of time (e.g., for the whole year or seasonal) assuming the worst-case meteorological conditions, [3,4]. Given that the SLR is not the most efficient technique, since the OHTL ampacity usually gets underrated, a new framework can be used for real-time calculation of the ampacity, namely the dynamic line rating (DLR), [5], where the measured external conditions (wind, ambient temperature or solar irradiation) are taken into account to obtain the line rating. Two major standards can be highlighted for thermal rating: IEEE, [4], and CIGRE, [6]. Although these standards are not directly oriented to the DLR approach, their thermal equations are usually used for the calculation of the ampacity in OHTLs, [7,8]. In this context the CIGRE guide has been considered in this work because, as studied in [9], the IEEE std. might represent a too conservative approach, reducing excessively the DLR with high wind speeds.

Regarding the measurements of the weather conditions used to obtain the DLR, information from weather stations has been considered by a remarkable number of studies, like that in [10], where the method is applied for the identification of critical spans, or the work in [11], analyzing direct and indirect measurements. Finally, some lines of investigation are oriented to the prediction of the DLR using forecasting techniques for the meteorological variables, [12].

As mentioned before, the ampacity is calculated so that the conductor temperature rises to a determined limit value, which might be established using different criteria, such as conductor deterioration or regulatory requirements for minimum electrical clearance. However, the real-time variability of the external conditions, produces a dynamic evolution of the conductor temperature, leading to a possible temporary violation of the defined limit.

In this research, the influence of the environmental conditions on the DLR is analyzed, and an alternative approach is proposed to obtain the ampacity of OHTLs considering the dynamic evolution of the conductor temperature. Even though the presented technique assumes a high frequency in the measurement gathering, a method is presented to correct the DLR when this information is not available.

The rest of the work is organized as follows: Section 2 presents the traditional calculation of the ampacity of OHTLs and the possible transient problems related to the conductor temperature. The proposed technique is presented in Section 3, while its application to a simulated scenario and a real dataset is included in Sections 4 and 5 respectively. The most relevant conclusions are included in Section 6.

2. Problem statement

In this section, a typically used method to obtain the ampacity of an OHTL is described, jointly with its potential problems in terms of minimum electrical clearance.

* Corresponding author.
E-mail address: mgcagigal@us.es (M.Á. González-Cagigal).

https://doi.org/10.1016/j.epsr.2022.108234
Received 28 March 2022; Received in revised form 25 May 2022; Accepted 25 June 2022
Available online 5 July 2022

2.1. Ampacity calculation

For a given conductor, the ampacity, I^{max}, is defined as the maximum current that can circulate permanently, so that the temperature of the conductor rises to a previously established limit value, T_c^{lim}, under a set of external meteorological conditions, namely:

- Ambient temperature, T_{amb} [°C].
- Wind speed, v_w [m/s].
- Wind direction w.r.t. the line span, characterized by the angle α_w [rad], e.g., $\pi/2$ for perpendicular wind.
- Solar radiation, I_s [W/m^2].

In order to calculate the value of I^{max}, the thermal equilibrium equation presented in [6],

$$P_r(T_c^{lim}) + P_c(T_c^{lim}) - P_s - P_J(T_c^{lim}, I^{max}) = 0, \tag{1}$$

must be satisfied under these ambient conditions, where P_r and P_c are respectively the radiative and convective heat losses, P_s is the solar heating and P_J is the Joule heating, which can be obtained as

$$P_J(T_c, I) = I^2 \cdot R_{AC}(T_c), \tag{2}$$

with $R_{AC}(T_c)$ being the AC resistance of the conductor at temperature T_c. Substituting (2) in (1), the following expression can be derived for the ampacity:

$$I^{max} = \sqrt{\frac{P_r(T_c^{lim}) + P_c(T_c^{lim}) - P_s}{R_{AC}(T_c^{lim})}}. \tag{3}$$

In the previous equation, the values of P_r, P_c and P_s for the temperature T_c^{lim} are calculated in this work according to the expressions provided by the CIGRE guide, [6].

2.2. Dynamic temperature evolution

The calculation of the ampacity given by Eq. (3) assumes constant external conditions during the corresponding time period, typically the mean values of the involved variables in a 10-min interval. Even though this assumption might be valid for some magnitudes, as the ambient temperature, other variables present a significant variation in this period. Take as an example the evolution of the wind speed in a 10-min interval, represented in Fig. 1, where real-time measurements from a weather station Froggit hp1000se PRO have been used.

For a given conductor with a thermal capacity c_p, the mentioned variability in the meteorological conditions produces a transient behavior in the temperature of the conductor, T_c, which can be described using the equation

$$m \cdot c_p \cdot \frac{dT_c}{dt} = P_r(T_c) + P_c(T_c) - P_s - P_J(T_c, I), \tag{4}$$

where m is the mass per unit length of the conductor. The reader may notice that, for constant meteorological conditions, the steady-state regime (null derivative) reduces to Eq. (1). However, under time-variant conditions, the temperature of the conductor can transiently exceed the established limit ($T_c > T_c^{lim}$), causing a temporary increase in the conductor sag which might produce a violation of the regulatory requirements for minimum electrical clearance.

2.3. Numerical example

In order to illustrate the described situation, the 10-min wind speed profile shown in Fig. 1 has been considered, while, for simplicity sake, the rest of the external conditions have been taken as constant values, summarized in Table 1. An aluminum conductor steel reinforced (ACSR) 455-54/7 (CONDOR) has been used, as a typical one in OHTLs, with an initial temperature of 50°C.

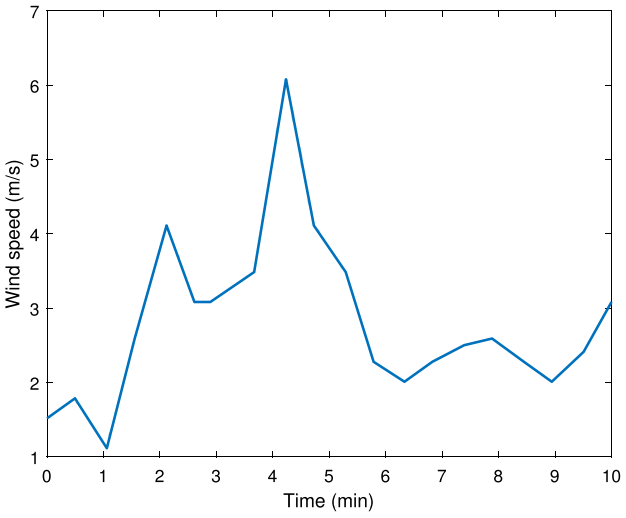

Fig. 1. Evolution of the wind speed in a 10-min period.

Table 1
External conditions in the numerical example.

Variable	Unit	Value
I_s	W/m^2	700
T_{amb}	°C	25
α_w	rad	$\pi/3$

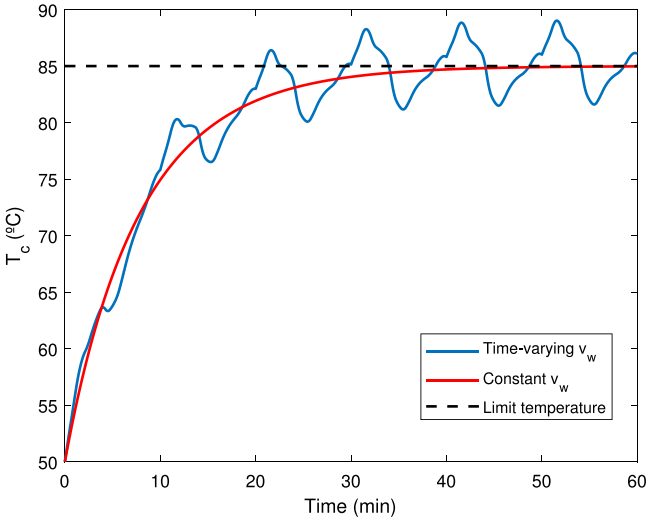

Fig. 2. Evolution of the conductor temperature in a 60-min period.

Fig. 2 represents the evolution of the conductor temperature during 60 min in two situations: considering a constant wind speed over time, equal to the mean value (in this example, $v_w = 2.79$ m/s), and assuming that the wind-speed profile presented in Fig. 1 is repeated 6 times.

In both cases it is considered that the current corresponds to the value of I^{max} calculated with Eq. (3) and a typical limit temperature $T_c^{lim} = 85$ °C ($I = I^{max} = 1541$ A).

It is observed how the value of T_c is higher than the limit in some moments during the 60-min interval, which might cause the violation of the minimum electrical clearance. In the next section, an alternative method is proposed to obtain a new value of I^{max} for which it is satisfied that the conductor temperature never exceeds the previously defined limit.

3. Proposed method

In this section, the new value of the ampacity will be calculated taking into account the dynamic evolution of the conductor temperature. Then a numerical example is presented to test the influence of the initial conditions in the results. Finally, a method is proposed for real-time applications.

3.1. Ampacity calculation

As previously mentioned, the value of I^{max} is typically calculated with Eq. (3), considering steady-state conditions for the variables involved. The alternative method proposed in this work takes into account the variability in the meteorological conditions and the thermal capacity of the conductor using the dynamic Eq. (4). This novel method to obtain the value of I^{max} is described below:

- First, the initial conductor temperature, T_{c0}, is selected. In the numerical example presented later in this section it will be shown how the influence of this initialization vanishes in time and does not affect the steady-state results.
- Using Eq. (4), the evolution of T_c during N_c cycles is calculated for each value of the current I. The profiles of the external conditions are repeated N_c times, this number being chosen to ensure that the total time is high enough, compared to the time constant $m \cdot c_p$ in the differential Eq. (4). In this manner, the periodic steady-state regime of the temperature T_c will be reached irrespective of the initial conditions taken, as will be proven in the subsequent numerical example, shown in Fig. 3, where the calculation process will be illustrated for a better comprehension.
- Finally, the ampacity corresponds to the value of I that satisfies the equality $\max(T_c) = T_c^{lim}$.

3.2. Numerical example

For the numerical example presented in the previous section, the new value of I^{max} is calculated using the proposed method. The number of 10-min cycles simulated is $N_c = 6$. Regarding the initial conductor temperature, different values have been used in order to verify how this initial condition has no influence on the calculated value of I^{max}. In all cases, the ampacity obtained is 1427 A, independently of the value of T_{c0}. Fig. 3 represents the evolution of T_c for $I = I^{max}$, and different initial conditions.

3.3. Application to reduced sampling rates

In the proposed ampacity calculation, it is assumed a high sampling frequency for the measurement gathering, for this reason, the value of I^{max} obtained through this method will be denoted as I_{hf}^{max} in the sequel. However, in real applications, this rate is typically much lower (e.g., 10 min between two consecutive measurements) and the information provided for the different magnitudes corresponds to their mean values during this period, so that the ampacity must be calculated using Eq. (3), which will be named as I_{lf}^{max}.

However, as it has been shown in Fig. 2, the value of I_{lf}^{max} might result in temporary violations of the conductor limit temperature and therefore the minimum electrical clearance, so that it needs to be corrected. In this work, when the sampling rate is not high enough, a method is proposed to consider the dynamic effect in the conductor temperature for the calculation of the maximum current, based on a coefficient c, which is calculated in simulated scenarios where this meteorological variability is taken into account and a high sampling frequency is considered to calculate the value of I_{hf}^{max}. For each time period k the ratio between the high and low frequency ampacities is calculated:

$$c_k = \frac{I_{hf,k}^{max}}{I_{lf,k}^{max}} \tag{5}$$

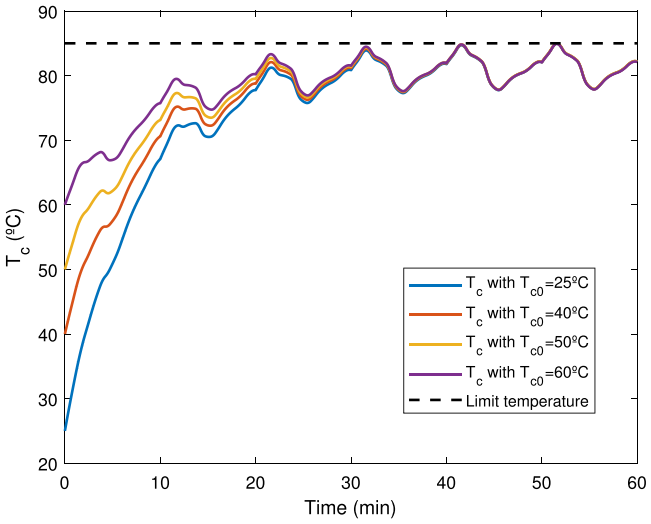

Fig. 3. Evolution of the conductor temperature using the proposed method and different initial conditions.

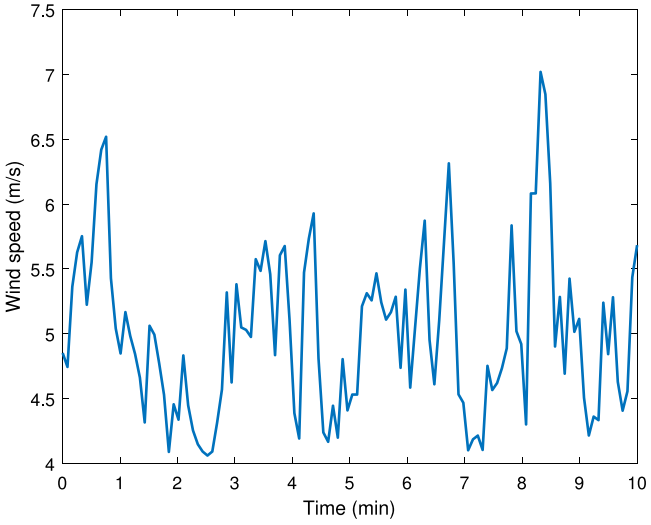

Fig. 4. Example of the considered SDE-based model for the wind speed.

In order to take an ampacity I^{max} as a conservative estimation of I_{hf}^{max}, a coefficient c is defined as the minimum of those coefficients for the total number of periods analyzed, N, yielding:

$$c = \min\left(c_k\right), \quad \text{with} \quad k = 1, \ldots, N \tag{6}$$

and

$$I^{max} = c \cdot I_{lf}^{max} \tag{7}$$

In the next section, a simulated scenario is presented where the value of this coefficient is obtained with different external conditions.

4. Simulated scenario

The previously defined coefficient c is calculated in a synthetic scenario where a set of independent 10-min time periods are simulated, with a sampling frequency of 0.1 Hz and the following considerations for the meteorological conditions:

- Constant values are taken for the ambient temperature, T_{amb}, and the solar radiation, I_s, since the variability of these magnitudes in a 10-min time interval can be neglected.

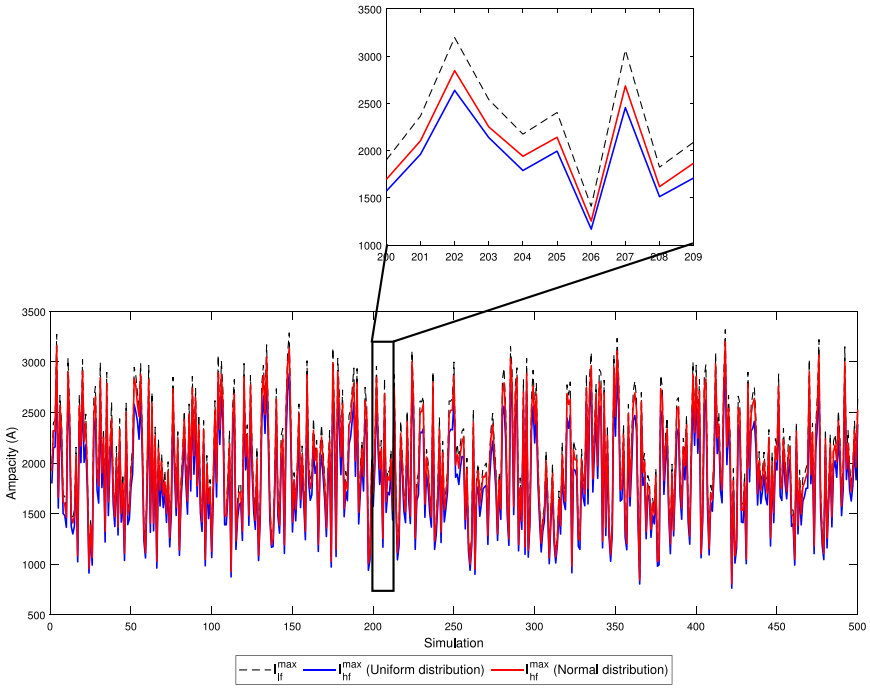

Fig. 5. Ampacities obtained in the Monte Carlo simulations.

- For the wind speed, a continuous-time model has been considered, based on stochastic differential equations (SDEs) and following, as proposed and validated in [13], a Weibull distribution. The mean value of this variable, $\overline{v}_w$, is previously assigned in each 10-min time interval as a uniformly distributed random variable with the range shown in Table 2. An example of this evolution for $\overline{v}_w = 5$ m/s is represented in Fig. 4.
- Finally, for the wind direction, the most unfavorable case has been assumed in terms of thermal refrigeration of the cable, so that a lower bound is obtained for the coefficient c and therefore, for the ampacity of the OHTL. As for the wind speed case, a SDE-based model is considered for the angle α_w. This variable is modeled in [14] using a Von Mises distribution, which has no analytic expression for its cumulative distribution function, so that it is not possible to obtain the corresponding SDE. Nevertheless, as the Von Mises distribution approaches to normal or uniform distributions in extreme cases, these approximations will be used in this work to look for bounds in the coefficient c for worst case scenarios: taking $\alpha_w \sim \mathbf{N}(\frac{\pi}{2}, \frac{\pi}{6})$ and $\alpha_w \sim \mathbf{U}(0, \pi)$. In both cases, the mean value of α_w in the 10-min period will be close to $\frac{\pi}{2}$ rad (optimal refrigeration angle), while the extreme values, 0 and π rad, are associated to a poor refrigeration.

First, an analysis is carried out using the ampacity calculated with high sampling frequency, I_{hf}^{max}, and low sampling frequency, I_{lf}^{max}. The involved variables are randomly assigned values within the ranges shown in Table 2, and the total number of Monte Carlo-based simulations was set to 60000. For a clearer representation, the ampacities obtained for the two distributions considered for the wind angle for a sample of only 500 simulations are represented in Fig. 5, including a zoomed plot with 10 simulations. In this graph it can be noticed how the value of I_{lf}^{max} is higher than I_{hf}^{max}, and the ampacity calculated with uniform distribution of the wind angle is lower than that considering a normal distribution.

Additionally, the quotient $c_k = I_{hf,k}^{max}/I_{lf,k}^{max}$ for both distributions is presented, in descending order, in Fig. 6 for the whole set of simulations. It is observed that the normal distribution provides higher values of the quotient c_k, while its minimum value, for the uniform distribution, is approximately 0.862, which would be taken as a lower bound of the coefficient c for the correction of I_{lf}^{max} in a real application.

Table 2
Range of the variables in the Monte Carlo-based simulations.

Variable	Unit	Range
I_s	W/m^2	[0 800]
T_{amb}	°C	[−10 50]
$\overline{v}_w$	m/s	[0.5 10]

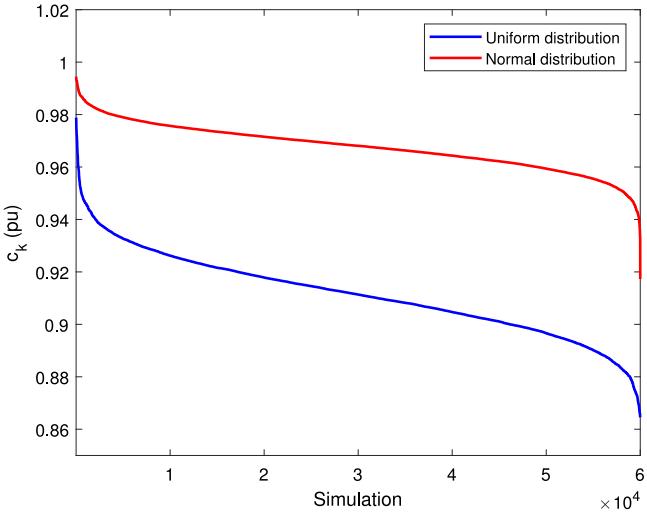

Fig. 6. Quotient c_k obtained for the Monte Carlo simulations.

Although the value taken in the previous scenario as low sampling frequency (one sample each 10 min) is a typical value provided by commercial weather stations (as that considered for the application included in Section 5), the Monte Carlo simulations carried out to obtain the coefficient c can consider different low sampling frequencies.

Table 3
Variation of the coefficient c with the sampling period of the weather station.

Sampling period (min)	Coefficient c (pu)
10	0.862
5	0.879
2	0.901
1	0.932

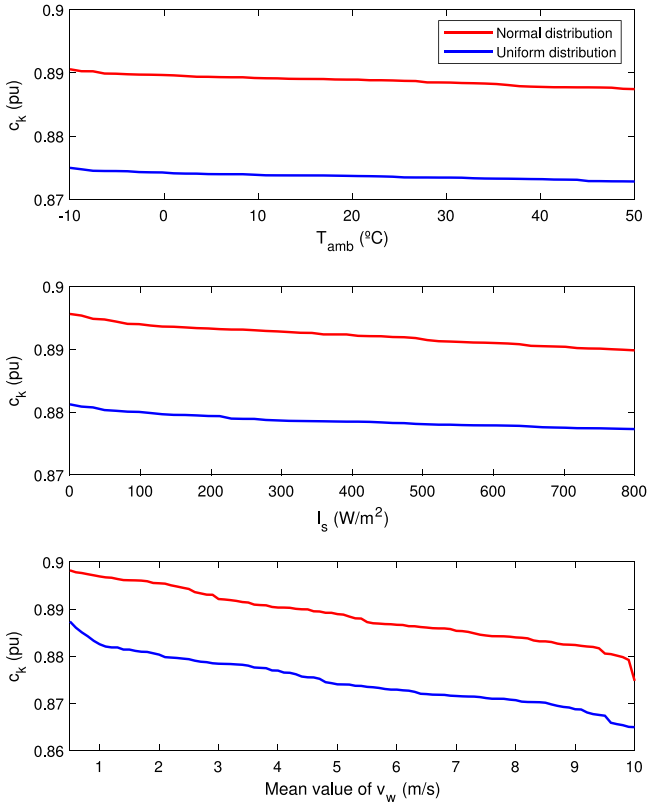

Fig. 7. Quotient c_k with variations of (a) T_{amb} (b) I_s (c) $\overline{v}_w$.

Fig. 8. Weather station Froggit hp1000se, [15].

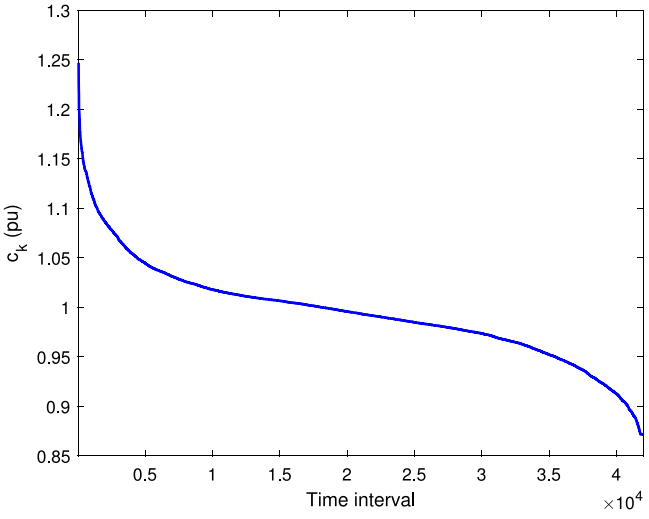

Fig. 9. Quotient c_k with real data.

Table 3 represents the values obtained for the coefficient c with different sampling periods. As expected, it can be noticed that, the value of c increases (resp. decreases) with the sampling frequency (resp. period), since the variability of the weather conditions between two consecutive samples is lower.

Finally, the individual influence of each variable in the coefficient c is subsequently analyzed. For a certain magnitude, it is assumed a variation within the range shown in Table 2. Fig. 7 presents the variation of c_k with the ambient temperature (Fig. 7a), the solar radiation (Fig. 7b) and the mean value of the wind speed (Fig. 7c). In all cases, the two distributions used for the wind direction has been compared, maintaining the assumption of the most unfavorable conditions.

It can be noticed that the variations of $\overline{v}_w$ have a higher influence on the coefficient c than those of the ambient temperature or the solar radiation for both the normal and the uniform distributions, with approximately 0.02 pu variation of the quotient c_k from $\overline{v}_w = 0.5$ m/s to $\overline{v}_w = 10$ m/s.

5. Application to real data

In the previous section, the value of the coefficient c was calculated in a simulated scenario where the most unfavorable conditions were assumed for the wind direction. In this section the results obtained will be validated using a real dataset from the previously mentioned weather station Froggit hp1000se (see Fig. 8).

For this weather station, the time between two consecutive measurements ranges from 20 to 25 s for each magnitude, so that the algorithm proposed in this work can be used to obtain the ampacity of the conductor, I_{hf}^{max}. For simplicity sake, it is assumed that the weather station angle reference is aligned with the line span under study, directly providing the angle α_w.

Additionally, the weather station used in this work also provides the mean values of the involved magnitudes in time intervals of 10 min, so that I_{lf}^{max} can be obtained, jointly with the quotient c_k, at instant k. Measurements obtained from a one-year period were preprocessed in order to remove bad data, yielding approximately a total number of 42000 valid periods of 10 min. Fig. 9 represents, in descending order, the values obtained for the quotient c_k. Two aspects can be highlighted from the graph:

- The values obtained with real data are, in most of the cases, higher than those from the simulated scenario. The reason is that the most unfavorable case was assumed in the synthetic scenario for the generation of the wind-direction profile.
- The minimum value of c_k (0.872) is very similar to that obtained in Section 4, so that the coefficient c, as defined in Eq. (6), approximately matches in both cases, giving evidence of the accuracy of the proposed method to correct the ampacity calculated with a reduced sampling rate.

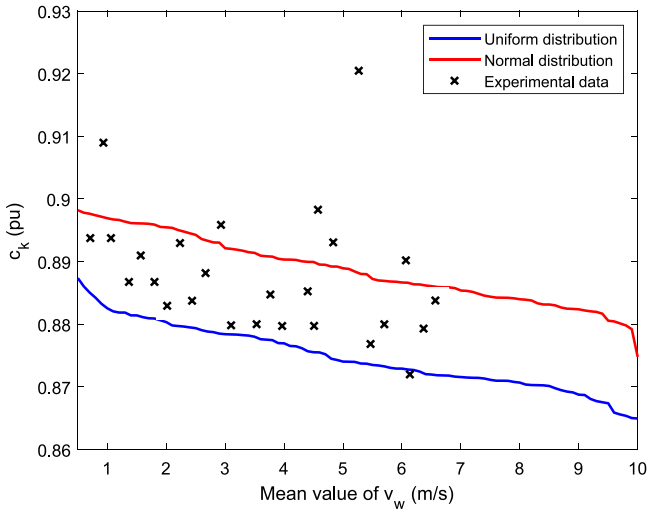

Fig. 10. Experimental c_k for different values of $\bar{v}_w$.

In the simulated scenarios presented in Section 4 it was observed that the mean value of the wind speed was the variable with the higher influence in the quotient c_k. In order to assess if the simulated results fit the real data in worst case scenarios, Fig. 10 shows the minimum values of c_k obtained for different mean values of the measured wind speed, where the synthetic curves presented in Fig. 7c are also represented as a reference.

It can be noticed that most experimental values remain between the normal and the uniform distributions, so that the latter can be considered to obtain a lower bound of the coefficient c.

6. Conclusion

In this work, it has been presented a method to calculate the maximum current which can permanently circulate through an overhead transmission line, taking into account the dynamic evolution of the conductor temperature, so that it never exceeds a previously established limit.

Additionally, a coefficient has been defined to correct the ampacity calculated in cases where only a reduced sampling rate (e.g., every 10 min) is available for the measurement gathering. For an ACSR 455-54/7 (CONDOR), a set of simulated cases have been considered with unfavorable external conditions so that a lower bound can be obtained for the mentioned coefficient. Finally, the validity of the results obtained has been assessed using a set of real measurements from a weather station, leading to a very similar minimum value (0.872) compared to the simulated one (0.862). The use of the proposed coefficient might prevent the violation of the regulatory requirements for minimum electrical clearance in OHTLs, reducing accordingly the derived risks.

CRediT authorship contribution statement

M.Á. González-Cagigal: Conceptualization, Methodology, Data curation, Writing – original draft, Writing – review & editing. **J.A. Rosendo-Macías:** Conceptualization, Methodology, Supervision, Writing – original draft, Writing – review & editing. **A. Bachiller-Soler:** Conceptualization, Methodology, Supervision, Writing – original draft, Writing – review & editing. **D. Señas-Sanvicente:** Conceptualization, Methodology, Writing – original draft, Writing – review & editing.

Declaration of competing interest

The authors declare that they have no known competing financial interests or personal relationships that could have appeared to influence the work reported in this paper.

Acknowledgments

The authors thank the research project HySGrid+ (CER-20191019) for the financial support.

References

[1] Babar Noor, M. Zulqarnain Abbasi, Shahryar Shafique Qureshi, Sanaullah Ahmed, Temperature and wind impacts on sag and tension of AAAC overhead transmission line, Int. J. Adv. Appl. Sci. 5 (2018) 14–18.
[2] N. Hayakawa, et al., Analysis of current limiting and recovery characteristics of superconducting fault current limiting transformer (SFCLT) with YBCO coated conductors, IEEE Trans. Appl. Superconduct. 21 (2011) 1422–1425.
[3] C.W.G. B2.12., Guide for selection of weather parameters for bare overhead conductor ratings, in: Technical Brochure, Vol. 299, 2006.
[4] IEEE standard for calculating the current-temperature relationship of bare overhead conductors, in: IEEE Std, Vol. 738–2012, 2013, pp. 1–72.
[5] S. Karimi, P. Musilek, A.M. Knight, Dynamic thermal rating of transmission lines: A review, Renew. Sustain. Energy Rev. 91 (C) (2018) 600–612.
[6] International council on large electric systems, CIGRE. Guide for thermal rating calculation of overhead lines, in: Technical Brochure 601, CIGRE, Paris, France, 2014.
[7] M. Maksić, G. Kosec, V. Djurica, A. Souvent, R. Trobec, Dynamic thermal rating of power lines in raining conditions - model and measurements, in: 2016 IEEE Power and Energy Society General Meeting, PESGM, 2016, pp. 1–4.
[8] L. Dawson, A.M. Knight, Applicability of dynamic thermal line rating for long lines, IEEE Trans. Power Deliv. 33 (2) (2018) 719–727.
[9] Mathew Simms, Lasantha Meegahapola, Comparative analysis of dynamic line rating models and feasibility to minimize energy losses in wind rich power networks, Energy Convers. Manag. 75 (2013) 11–20.
[10] Saifal Talpur, T.T. Lie, R. Zamora, Application of dynamic thermal rating: Overhead line critical spans identification under weather dependent optimized sensor placement, Electric Power Syst. Res. 180 (2020) 106125.
[11] David L. Alvarez, F. Faria da Silva, Enrique E. Mombello, Claus Leth Bak, Javier A. Rosero, Daníel Leólason, An approach to dynamic line rating state estimation at thermal steady state using direct and indirect measurements, Electr. Power Syst. Res. 163 (Part B) (2018) 599–611.
[12] S. Uski, Dynamic line rating forecastability for conservative day-ahead line rating values, in: IECON 2015-41st Annual Conference of the IEEE Industrial Electronics Society, 2015, pp. 003738–003742.
[13] Rafael Zárate-Miñano, Marian Anghel, Federico Milano, Continuous wind speed models based on stochastic differential equations, Appl. Energy 104 (2013) 42–49.
[14] T. Ringelband, P. Schäfer, A. Moser, Probabilistic ampacity forecasting for overhead lines using weather forecast ensembles, Electr. Eng. 95 (2013) 99–107.
[15] Froggit website. Available online: https://www.froggit.de.